

Synthesis, Characterization, and Crystal Structures of Dioxomolybdenum(VI) Complexes with O,N,N Type Tridentate Hydrazone Ligands as Catalyst for Oxidation of Olefins¹

W. G. Zhang^{a,*} and J. H. Liang^b

^aCollege of Chemistry and Chemical Engineering, Qiqihar University, Qiqihar, 161006 P.R. China

^bLibrary, Qiqihar University, Qiqihar, 161006 P.R. China

*e-mail: zhangweiguang1230@163.com

Received April 1, 2016

Abstract—The preparation of Mo(VI) hydrazone complexes, *cis*-[MoO₂L¹(CH₃OH)] (**I**) and *cis*-[MoO₂L²(CH₃OH)] (**II**), derived from *N*'-(3-bromo-2-hydroxybenzylidene)-2-chlorobenzohydrazide (H₂L¹) and *N*'-(3-bromo-2-hydroxybenzylidene)-4-bromobenzohydrazide (H₂L²), respectively, is reported. The complexes were characterized by elemental analyses, infrared and electronic spectroscopy, and single crystal structure analysis (CIF files CCDC nos. 1426875 (**I**), 1426871 (**II**)). The Mo atoms are coordinated by two *cis* terminal oxygen, ONO from the hydrazone ligand, and methanol oxygen. Even though the hydrazone ligands and the coordination sphere in both complexes are similar, the unit cell dimensions and the space groups are different. Complex **I** crystallized as orthorhombic space group *Pca*2₁ with unit cell dimensions *a* = 27.887(2), *b* = 8.0137(7), *c* = 15.544(1) Å, *V* = 3473.8(5) Å³, *Z* = 8, *R*₁ = 0.0450, *wR*₂ = 0.0539. Complex **II** crystallized as triclinic space group *P*1, with unit cell dimensions *a* = 8.2124(4), *b* = 8.5807(5), *c* = 12.9845(8) Å, α = 83.366(2)°, β = 79.201(2)°, γ = 80.482(2)°, *V* = 883.03(9) Å³, *Z* = 2, *R*₁ = 0.0278, *wR*₂ = 0.0569. The complexes were tested as catalyst for the oxidation of olefins, and showed effective activity.

Keywords: *cis*-dioxomolybdenum(VI) complexes, hydrazone ligands, catalysis, oxidation, olefins

DOI: 10.1134/S1070328417060100

INTRODUCTION

Molybdenum is an essential metal that is capable of forming metal complexes with various ligands [1–5]. Molybdenum is not only much less toxic than many other metals of industrial importance but it is also an essential constituent of certain enzymes that catalyze reduction of molecular nitrogen and nitrate in plants and oxidation (hydroxylation) of xanthine and other purines and aldehydes in animals [6]. Epoxides are very important chemicals for manufacturing a range of important commercial products such as pharmaceuticals and polymers. Many transition metal complexes have been reported for oxidation of olefins [7–13]. Molybdenum complexes are known for considerable use in organic chemistry, in particular for the various oxidations of organic compounds [4, 14, 15]. Oxido-peroxido molybdenum complexes have been intensively investigated as oxidation catalysts for variety of organic substrates, particularly for sulfoxidation and epoxidation of olefins [16–19]. In order to further study the catalytic potentiality of the oxido-peroxido complexes of molybdenum, in this paper, the synthesis, crystal structures and catalytic activity of Mo(VI)

hydrazone complexes, *cis*-[MoO₂L¹(CH₃OH)] (**I**) and *cis*-[MoO₂L²(CH₃OH)] (**II**), derived from *N*'-(3-bromo-2-hydroxybenzylidene)-2-chlorobenzohydrazide (H₂L¹) and *N*'-(3-bromo-2-hydroxybenzylidene)-4-bromobenzohydrazide (H₂L²), respectively, are reported.

EXPERIMENTAL

Materials and methods. All the reagents and solvents used in the synthesis were procured commercially and used without subsequent purification. The starting material, bis(acetylacetonato) dioxomolybdenum(VI), [MoO₂(Acac)₂] was prepared as described in the literature [20]. Microanalyses (C, H, N) were performed using a Perkin-Elmer 2400 elemental analyzer. Infrared spectra were carried out using the JASCO FT-IR model 420 spectrophotometer with KBr disk in the region 4000–400 cm^{−1}. Electronic absorption spectra measurement in acetonitrile was measured using a Shimadzu 1650 UV-Vis spectrophotometer. ¹H and ¹³C NMR spectra were measured in DMSO-d⁶ on Bruker 300 MHz and 75 MHz NMR spectrometer.

¹ The article is published in the original.

Synthesis of H_2L^1 . 0.201 g (1.0 mmol) of 3-bromosalicylaldehyde in 20 mL methanol was added to 20 mL of 0.170 g (1.0 mmol) of 2-chlorobenzohydrazide. The solution mixture was refluxed with vigorous stirring for 2 h. The solvent was then evaporated and allowed to cool to room temperature. The white precipitate was filtered and washed with methanol and dried in air. The yield was 86%.

For $C_{14}H_{10}N_2O_2ClBr$

anal. calcd., %: C, 47.55; H, 2.85; N, 7.92.
Found, %: C, 47.32; H, 2.96; N, 8.04.

IR (KBr; ν_{\max} , cm^{-1}): 3441 w $\nu(\text{OH})$, 1659 s $\nu(\text{C}=\text{O})$, 1591 w $\nu(\text{C}=\text{N})$, 1545 m $\nu(\text{Ar}-\text{O})$, 1296 m $\nu(\text{C}-\text{O})$. ^1H NMR (DMSO- d^6 ; δ , ppm): 6.95 (t., 1H, ArH), 7.39–7.72 (m., 6H, ArH), 8.69 (s., 1H, $\text{CH}=\text{N}$), 10.27 (s., 1H, NH), 12.31 (s., 1H, OH). ^{13}C NMR (DMSO- d^6 ; δ , ppm): 111.9, 120.3, 121.8, 127.3, 129.2, 130.5, 131.7, 133.0, 133.9, 134.3, 135.7, 147.2, 159.2, 164.5.

Synthesis of H_2L^2 . 0.201 g (1.0 mmol) of 3-bromosalicylaldehyde in 20 mL methanol was added to 20 mL of 0.215 g (1.0 mmol) of 4-bromobenzohydrazide. The solution mixture was refluxed with vigorous stirring for 2 h. The solvent was then evaporated and allowed to cool to room temperature. The white precipitate was filtered and washed with methanol and dried in air. The yield was 83%.

For $C_{14}H_{10}N_2O_2Br_2$

anal. calcd., %: C, 42.24; H, 2.53; N, 7.04.
Found, %: C, 42.11; H, 2.62; N, 6.96.

IR (KBr; ν_{\max} , cm^{-1}): 3445 w $\nu(\text{OH})$, 1657 s $\nu(\text{C}=\text{O})$, 1590 w $\nu(\text{C}=\text{N})$, 1545 m $\nu(\text{Ar}-\text{O})$, 1292 m $\nu(\text{C}-\text{O})$. ^1H NMR (DMSO- d^6 ; δ , ppm): 6.95 (t., 1H, ArH), 7.40 (d., 1H, ArH), 7.62 (d., 1H, ArH), 7.77–7.94 (m., 4H, ArH), 8.70 (s., 1H, $\text{CH}=\text{N}$), 10.63 (s., 1H, NH), 12.17 (s., 1H, OH). ^{13}C NMR (DMSO- d^6 , δ ppm): 111.9, 120.3, 121.9, 126.1, 128.9, 130.5, 131.3, 132.2, 133.5, 147.0, 159.2, 164.2.

Synthesis of *cis*-[$\text{MoO}_2\text{L}^1(\text{CH}_3\text{OH})$] (I). 0.328 g (1.0 mmol) of $\text{MoO}_2(\text{Acac})_2$ in 20 mL of methanol was mixed with 20 mL of 0.354 g (1.0 mmol) of H_2L^1 . The solution mixture was then refluxed with vigorous stirring for 1 h. After leaving the solution for a few days at room temperature, fine orange crystals were formed. The product was filtered and washed with methanol. The yield was 51%.

For $C_{15}H_{12}N_2O_5ClBrMo$

anal. calcd., %: C, 35.22; H, 2.36; N, 5.48.
Found, %: C, 35.40; H, 2.28; N, 5.37.

IR (KBr; ν_{\max} , cm^{-1}): 1611 m $\nu(\text{C}=\text{N})$, 1440 m $\nu(\text{C}=\text{C})$, 1371 m $\nu(\text{Ar}-\text{O})$, 1159 s $\nu(\text{C}-\text{O})$, 1079 s, 951 s, 850 s $\nu(\text{Mo}=\text{O})$.

Synthesis of *cis*-[$\text{MoO}_2\text{L}^2(\text{CH}_3\text{OH})$] (II). 0.328 g (1.0 mmol) of $\text{MoO}_2(\text{Acac})_2$ in 20 mL of methanol was mixed with 20 mL of 0.398 g (1.0 mmol) of H_2L^2 . The solution mixture was then refluxed with vigorous stirring for 1 h. After leaving the solution for a few days at room temperature, fine orange crystals were formed. The product was filtered and washed with methanol. The yield was 45%.

For $C_{15}H_{12}N_2O_5Br_2Mo$

anal. calcd., %: C, 32.40; H, 2.18; N, 5.04.
Found, %: C, 32.53; H, 2.25; N, 4.96.

IR (KBr; ν_{\max} , cm^{-1}): 1610 m $\nu(\text{C}=\text{N})$, 1445 m $\nu(\text{C}=\text{C})$, 1368 m $\nu(\text{Ar}-\text{O})$, 1159 s $\nu(\text{C}-\text{O})$, 1073 s, 947 s, 852 s $\nu(\text{Mo}=\text{O})$.

X-ray structure determination. X-ray measurements were performed using a Bruker Smart 1000 CCD diffractometer with graphite monochromated MoK_α radiation ($\lambda = 0.71073 \text{ \AA}$) using the ω -scan technique. Determination of the Laue class, orientation matrix, and cell dimensions were performed according to the established procedures where Lorentz polarization and absorption corrections were applied. Absorption corrections were applied by fitting a pseudoellipsoid to the ψ -scan data of selected strong reflections over a wide range of 2θ angles [21]. The positions of almost all non-hydrogen atoms were located with direct methods. Subsequent Fourier syntheses were used to locate the remaining non-hydrogen atoms. All non-hydrogen atoms were refined anisotropically. The methanol H atoms in the complexes were located from difference Fourier maps and refined isotropically, with O–H distances restrained to 0.85(1) \AA . The remaining hydrogen atoms were placed in calculated positions and constrained to ride on their parent atoms. The analysis was performed with the aid of the SHELXS-97 and SHELXL-97 suite of codes [22, 23]. The crystallographic data for the complexes are summarized in Table 1. Selected bond lengths and angles are given in Table 2. Hydrogen bonds are listed in Table 3.

Supplementary material for structures has been deposited with the Cambridge Crystallographic Data Centre (CCDC nos. 1426875 (I), 1426871 (II); deposit@ccdc.cam.ac.uk or <http://www.ccdc.cam.ac.uk>).

Catalytic epoxidation of olefins. In a typical catalytic experiment, TBHP (1 mmol) was added to a solution of olefin (1 mmol), chlorobenzene (1 mmol) as an internal standard and the complexes (2×10^{-4} mmol) in 1,2-dichloroethane (0.5 mL). The mixture was stirred at

Table 1. Crystallographic data and structure refinement for **I** and **II**

Parameter	Value	
	I	II
Formula weight	511.6	556.0
Crystal system	Orthorhombic	Triclinic
Space group	<i>Pca2</i> ₁	<i>P</i> ₁
<i>a</i> , Å	27.887(2)	8.2124(4)
<i>b</i> , Å	8.0137(7)	8.5807(5)
<i>c</i> , Å	15.544(1)	12.9845(8)
α, deg	90	83.366(2)
β, deg	90	79.201(2)
γ, deg	90	80.482(2)
<i>V</i> , Å ³	3473.8(5)	883.03(9)
<i>Z</i>	8	2
μ(Mo <i>K</i> _α), mm ⁻¹	3.238	5.296
ρ _{calcd} , g cm ⁻³	1.956	2.091
<i>T</i> , K	298(2)	298(2)
<i>F</i> (000)	2000	536
Crystal size, mm	0.28 × 0.28 × 0.26	0.31 × 0.27 × 0.27
θ Range, deg	2.54–25.09	2.42–25.50
Index ranges	−28 ≤ <i>h</i> ≤ 33, −9 ≤ <i>k</i> ≤ 9, −18 ≤ <i>l</i> ≤ 18	−9 ≤ <i>h</i> ≤ 9, −10 ≤ <i>k</i> ≤ 10, −15 ≤ <i>l</i> ≤ 15
<i>T</i> _{min} / <i>T</i> _{max}	0.4642/0.4865	0.2906/0.3289
Reflections collected	30357	8258
Observed reflections (<i>I</i> > 2σ(<i>I</i>))	4089	2724
Data/restraints/parameters	6178/3/459	3253/1/230
Goodness of fit on <i>F</i> ²	1.000	1.019
<i>R</i> _{int}	0.1092	0.0225
Final <i>R</i> indices (<i>I</i> > 2σ(<i>I</i>))	0.0450, 0.0539	0.0278, 0.0569
<i>R</i> indices (all data)	0.1046, 0.0639	0.0393, 0.0610
Largest peak and hole, <i>e</i> Å ⁻³	0.567 and −0.479	0.515 and −0.554

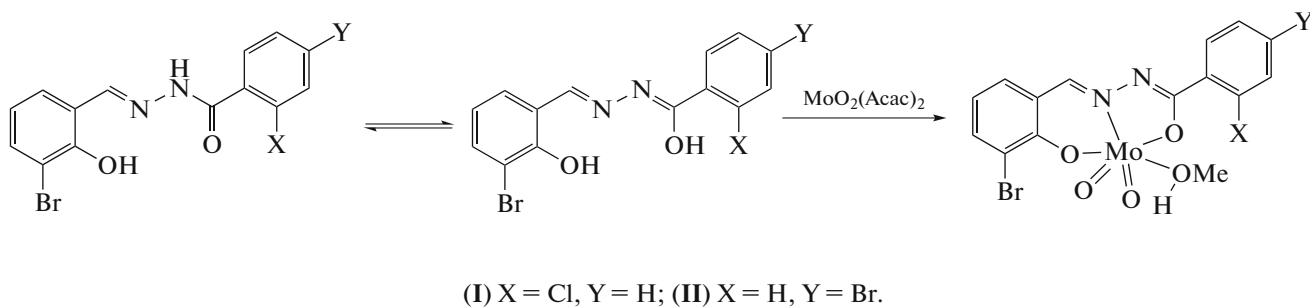
80°C under air and the course of the reaction was monitored using gas chromatography (Agilent Technologies Instruments 6890N, equipped with a capillary column (19019J-413 HP-5, 5% Phenyl Methyl Siloxane, Capillary 60.0 m × 250 μm × 1.00 μm) and a flame ionization detector). Assignments of products were made by comparison with authentic samples. All the reactions were run two times.

RESULTS AND DISCUSSION

The hydrazone ligands were reacted with bis(acetylacetonato)dioxomolybdenum(VI) in methanol solution under refluxing conditions, generating fine crystalline complexes, as shown in Scheme:

Table 2. Selected bond lengths (Å) and angles (deg) for **I** and **II**

Bond	<i>d</i> , Å	Bond	<i>d</i> , Å
I			
Mo(1)–O(1)	1.935(4)	Mo(1)–O(2)	2.017(4)
Mo(1)–N(1)	2.231(6)	Mo(1)–O(3)	2.305(4)
Mo(1)–O(4)	1.680(4)	Mo(1)–O(5)	1.698(4)
Mo(2)–O(6)	1.931(4)	Mo(2)–O(7)	2.031(4)
Mo(2)–N(3)	2.245(6)	Mo(2)–O(8)	2.289(5)
Mo(2)–O(9)	1.684(4)	Mo(2)–O(10)	1.694(5)
II			
Mo(1)–O(1)	1.924(2)	Mo(1)–O(2)	2.019(2)
Mo(1)–N(1)	2.232(2)	Mo(1)–O(3)	2.354(2)
Mo(1)–O(4)	1.698(2)	Mo(1)–O(5)	1.682(3)
Angle	ω , deg	Angle	ω , deg
I			
O(4)Mo(1)O(5)	105.9(2)	O(4)Mo(1)O(1)	97.9(2)
O(5)Mo(1)O(1)	104.6(2)	O(4)Mo(1)O(2)	97.4(2)
O(5)Mo(1)O(2)	97.6(2)	O(1)Mo(1)O(2)	148.25(18)
O(4)Mo(1)N(1)	93.4(2)	O(5)Mo(1)N(1)	159.03(19)
O(1)Mo(1)N(1)	80.36(18)	O(2)Mo(1)N(1)	71.15(19)
O(4)Mo(1)O(3)	171.3(2)	O(5)Mo(1)O(3)	82.7(2)
O(1)Mo(1)O(3)	81.16(18)	O(2)Mo(1)O(3)	79.51(18)
N(1)Mo(1)O(3)	77.95(19)	O(9)Mo(2)O(10)	105.3(2)
O(9)Mo(2)O(6)	98.6(2)	O(10)Mo(2)O(6)	105.1(2)
O(9)Mo(2)O(7)	95.1(2)	O(10)Mo(2)O(7)	97.2(2)
O(6)Mo(2)O(7)	149.53(18)	O(9)Mo(2)N(3)	93.7(2)
O(10)Mo(2)N(3)	158.8(2)	O(6)Mo(2)N(3)	80.51(19)
O(7)Mo(2)N(3)	71.5(2)	O(9)Mo(2)O(8)	170.8(2)
O(10)Mo(2)O(8)	83.2(2)	O(6)Mo(2)O(8)	82.35(18)
O(7)Mo(2)O(8)	80.03(18)	N(3)Mo(2)O(8)	77.4(2)
II			
O(5)Mo(1)O(4)	105.88(12)	O(5)Mo(1)O(1)	100.62(11)
O(4)Mo(1)O(1)	103.44(10)	O(5)Mo(1)O(2)	96.38(11)
O(4)Mo(1)O(2)	96.79(10)	O(1)Mo(1)O(2)	148.74(9)
O(5)Mo(1)N(1)	95.00(11)	O(4)Mo(1)N(1)	157.17(11)
O(1)Mo(1)N(1)	81.16(9)	O(2)Mo(1)N(1)	71.33(8)
O(5)Mo(1)O(3)	171.01(10)	O(4)Mo(1)O(3)	82.18(10)
O(1)Mo(1)O(3)	80.97(9)	O(2)Mo(1)O(3)	78.44(9)
N(1)Mo(1)O(3)	76.43(8)		



Scheme 1.

Crystals of the complexes are stabilized in air at room temperature, and soluble in methanol, ethanol, and acetonitrile. The molar conductance values of complexes **I** and **II** in methanol at concentration of 10^{-4} mol/L are 17 and $14 \Omega^{-1} \text{cm}^2 \text{mol}^{-1}$ indicating they are non-electrolytes [24].

The molecular structures of the complexes are shown in Fig 1. The asymmetric unit of **I** contains two independent dioxomolybdenum complex molecules. Structures of the dioxomolybdenum complex molecules of **I** and **II** are very similar to each other, except for the substituent groups of the benzohydrazine ligands. In each of the complexes, the coordination geometry around the Mo atom can be described as slightly distorted octahedron with the equatorial plane defined by one phenolic O, one imino N, and one enolic O atoms of the dianionic hydrazone ligand, and one oxo O atom, and with the two axial positions occupied by one O atom of a methanol ligand and the other oxo O atom. The hydrazone ligands coordinate to Mo atoms in meridional fashion forming five- and sixmembered chelate rings with bite angles of $71.2(2)^\circ$ and $80.4(2)^\circ$ (Mo(1) molecule), and $71.5(2)^\circ$ and $80.5(2)^\circ$ (Mo(2) molecule) for **I**, and $71.33(8)^\circ$ and $81.16(9)^\circ$ for **II**. The dihedral angles between the two substituted benzene rings of the hydrazone ligands are $10.5(5)^\circ$ (Mo(1) molecule) and $12.4(5)^\circ$ (Mo(2) mol-

ecule) for **I**, and $9.5(3)^\circ$ for **II**. The displacements of the Mo atoms from the equatorial mean planes toward the axial oxo atoms are $0.313(3) \text{ \AA}$ (Mo(1) molecule) and $0.298(3) \text{ \AA}$ (Mo(2) molecule) for **I**, and $0.338(2) \text{ \AA}$ for **II**. The hydrazone ligands are coordinated in their dianionic forms, which are evident from the N–C and O–C bond lengths, indicating the presence of the enolate form of the ligand amide groups. The Mo–O, Mo–N, and Mo=O bonds are within normal ranges and are similar to those observed in similar dioxomolybdenum(VI) complexes [25, 26].

In the crystal of **I**, the complex molecules are linked by methanol ligands through intermolecular O–H…N hydrogen bonds (Table 3) to form dimers. The dimers are further linked via weak Br…O interactions to form 2D network along the xy plane (Fig. 2a). In the crystal of **II**, adjacent complex molecules are linked by two methanol molecules through two intermolecular O–H…N hydrogen bonds (Table 3) to form a dimer (Fig. 2b). The dimers are further linked via weak Br…Br interactions to form 1D chains (Fig. 2b).

The weak and broad bands in the range 3350 – 3500 cm^{-1} for the ligands and the complexes can be assigned to the $\nu(\text{OH})$ vibrations. The Mo=O stretching modes occur as a pair of sharp strong bands at about 950 and 850 cm^{-1} for the complexes, which are

Table 3. Distances (Å) and angles (deg) involving hydrogen bonding of **I** and **II***

D–H…A	Distance, Å			Angle D–H…A, deg
	D–H	H…A	D…A	
I				
O(8)–H(8)…N(2) ⁱ	0.85(1)	1.93(3)	2.757(8)	164(8)
O(3)–H(3)…N(4) ⁱⁱ	0.85(1)	1.91(2)	2.740(7)	165(8)
II				
O(3)–H(3)…N(2) ⁱⁱⁱ	0.90(1)	1.88(1)	2.761(3)	171(4)

* Symmetry codes: ⁱ $1/2 - x, 1 + y, -1/2 + z$; ⁱⁱ $1/2 - x, -1 + y, 1/2 + z$; ⁱⁱⁱ $-x, 2 - y, -z$.

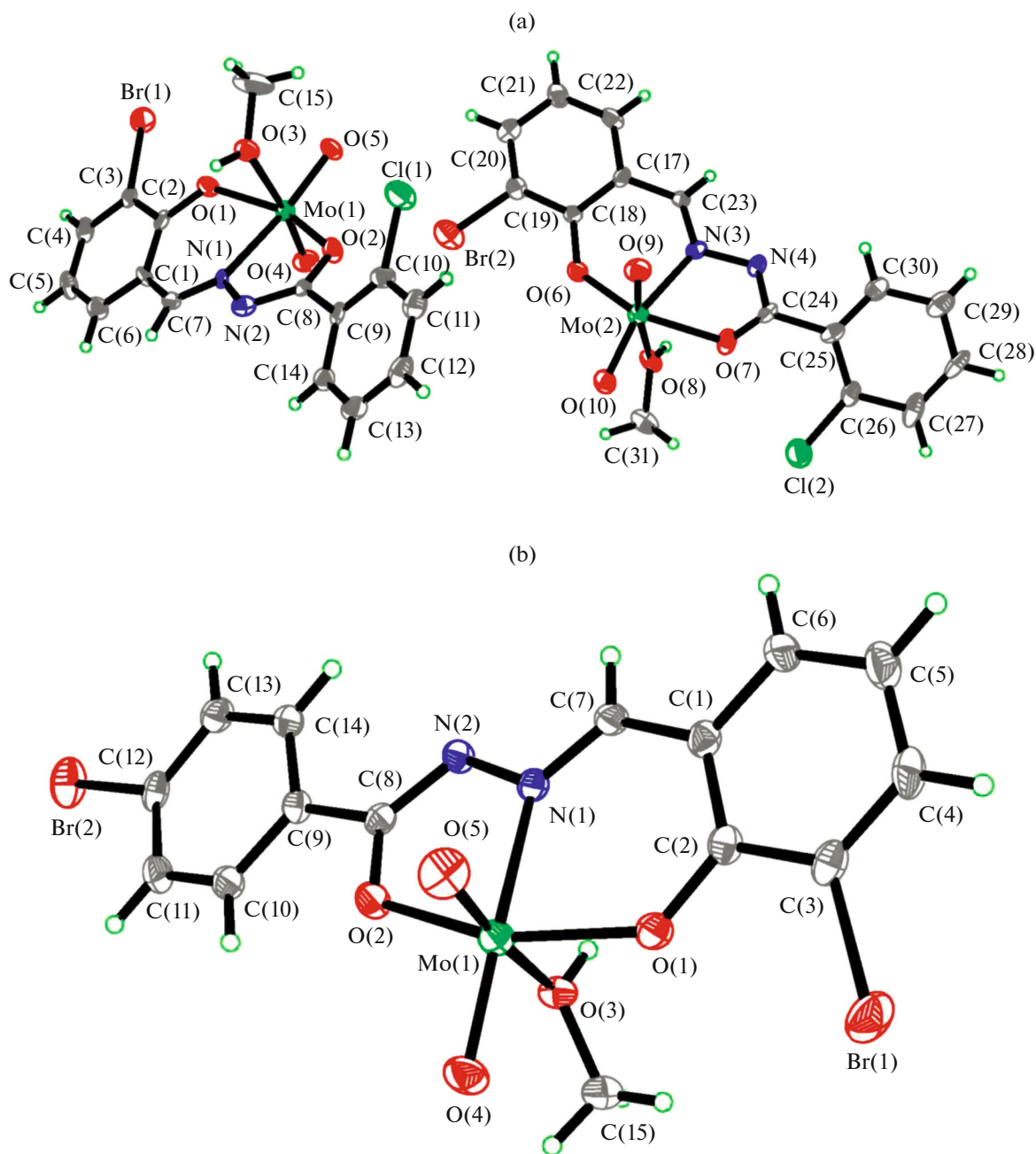


Fig. 1. Molecular structure of **I** (a) and **II** (b) with atom labeling scheme and 30% probability thermal ellipsoids for all non-hydrogen atoms.

assigned to the anti-symmetric and symmetric stretching modes of the dioxomolybdenum(VI) moieties. The bands due to the $\nu(\text{C}=\text{O})$ and $\nu(\text{NH})$ of the hydrazones were absent in the complexes, and new $\text{C}-\text{O}$ stretches appear at 1159 cm^{-1} for the complexes. This suggests occurrence of keto-imine tautomerization of the hydrazone ligands during coordination. The strong bands indicative of the $\text{C}=\text{N}-\text{N}=\text{C}$ groups in the complexes are shifted to 1611 cm^{-1} for **I** and 1610 cm^{-1} for **II**. The new weak peaks observed in the

range $400-800\text{ cm}^{-1}$ may be attributed to the $\text{Mo}-\text{O}$ and $\text{Mo}-\text{N}$ vibrations in the complexes. The IR spectra of the complexes are similar to each other, indicating the complexes are similar structures, as evidenced by the single crystal X-ray determination.

Considering the structures of two complexes are similar, the present work used complex **I** as catalyst to explore suitable experimental conditions. The catalytic property of complex **I** was first studied in the homogeneous epoxidation of cyclohexene, used as a

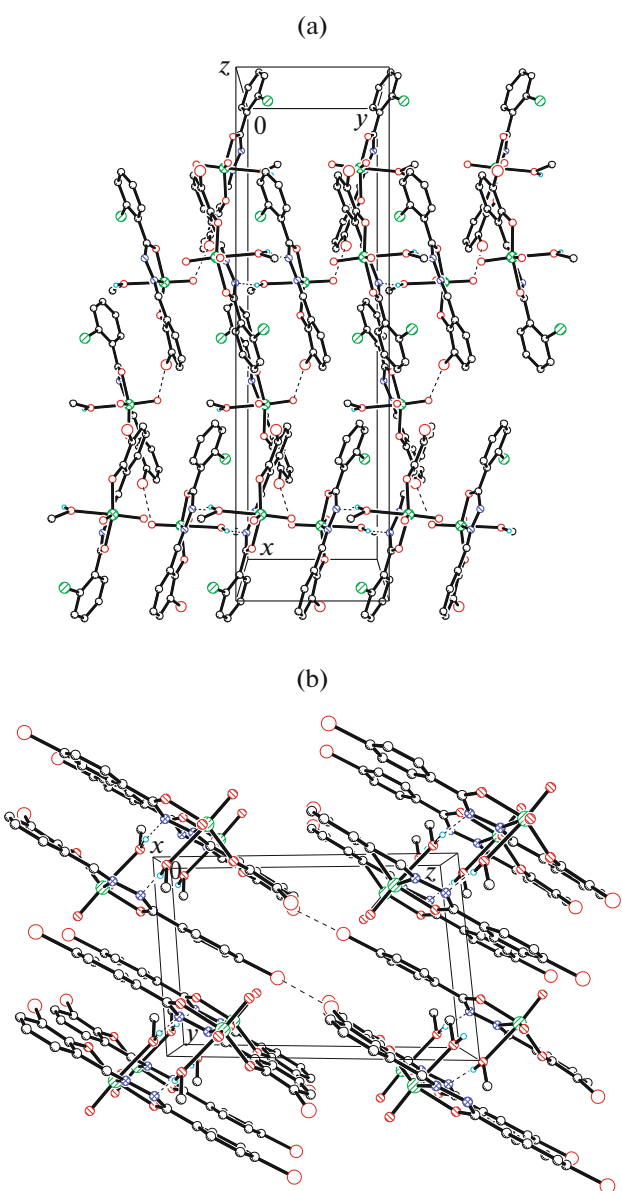


Fig. 2. Molecular packing diagram of **I** (a) viewed along the *z* axis and **II** (b) viewed along the *x* axis. Hydrogen bonds are shown as dashed lines.

Table 4. The solvent effects on the catalytic epoxidation of cyclohexene with TBHP using complex **I** as the catalyst*

Entry	Solvent	Conversion	Time	TON***
1	MeOH	87**	1 h	3700
2	EtOH	90**	1 h	4360
3	MeCN	95	1 h	4450
4	Cyclohexane	93**	1 h	4500
5	Toluene	97	1 h	4750
6	1,2-Dichloroethane	100**	30 min	5100
		95**	20 min	4900
		85**	5 min	4300

* The molar ratio for the complex : cyclohexene : TBHP is 1 : 5000 : 5000. The reactions were carried out at 80°C.

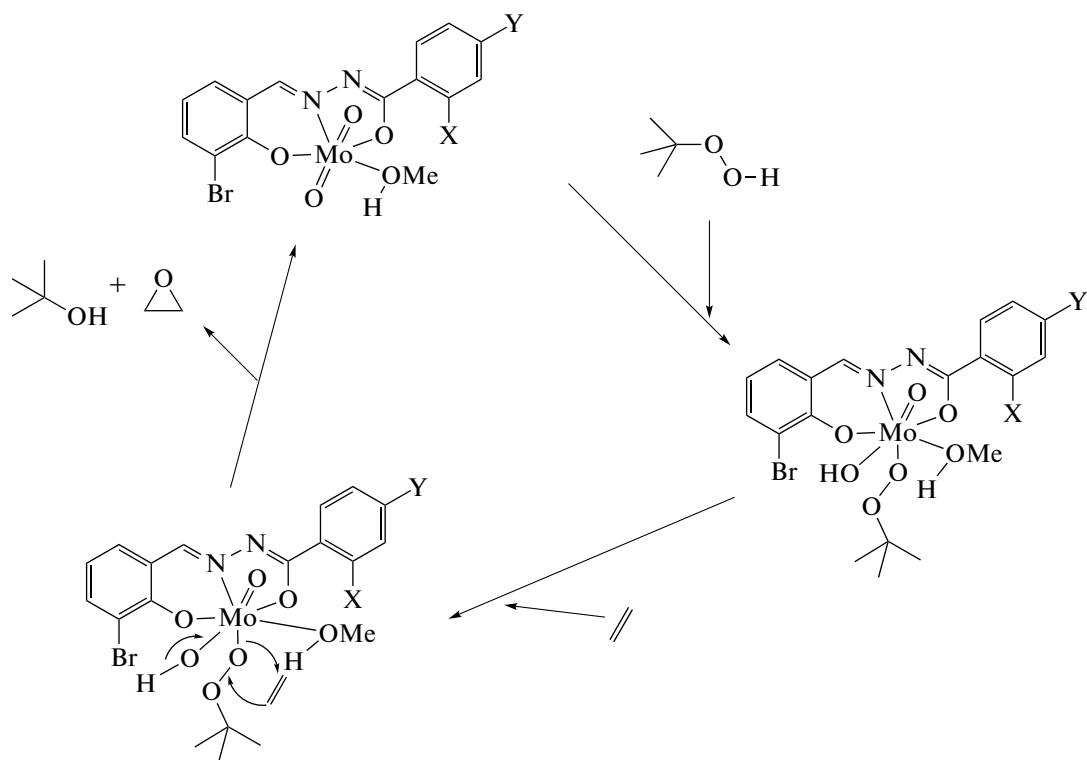
** The reactions were carried out at reflux.

*** TON = mmol of product/mmol of catalyst.

model substrate, and *tert*-butyl hydrogen peroxide (TBHP) as the oxygen donor. The influence of several solvents was evaluated (Table 4). It is clear that toluene and 1,2-dichloroethane produce the highest yields and the catalytic activity is the best when 1,2-dichloroethane was used as the solvent. At 80°C with 1,2-dichloroethane, a turnover number (TON) of 5100 with the complex can be achieved. So, 1,2-dichloroethane can be used as solvent in the catalyst experiment.

The catalytic epoxidation of some olefins using the complexes as catalyst is summarized in Table 5. In general, both complexes show similar catalytic properties. It is clear that the epoxide yields and selectivity are good for cyclohexene in only 30 min (entries 1 and 2). However, the catalytic property decreased for styrene, *p*-chlorostyrene, *p*-bromostyrene, *p*-methylstyrene, and substituted styrene. The electronic effects may play key roles in the catalytic process. The catalytic property of *p*-chlorostyrene and *p*-bromostyrene is better than styrene, while *p*-methylstyrene is lower than styrene (entries 3–10). The complexes were highly selective for the epoxide for cyclohexene, but lower for various styrenes with substituted benzaldehyde and acetophenone as side products.

In general, the mechanisms proposed for *t*-BuOOH-based epoxidation of olefins with Mo(VI) complexes are heterolytic in nature, involving coordination of the oxidant to the metal center [27]. The Lewis acidity of the Mo center increases the oxidizing power of the peroxy group and the olefin is subsequently deoxidized by nucleophilic attack on an electrophilic oxygen atom of the coordinated *tert*-butyl peroxide [28]. The proposed mechanism of catalytic epoxidation of olefins with TBHP catalyzed by the complexes is shown in Scheme 2:



Scheme 2.

Table 5. Catalytic oxidation results*

Entry	Substrate	Product	Compound	Time, min	Conversion, %	Selectivity, %	TON
1			I	30	100	100	5100
2			II	30	100	100	5200
3			I	60	63	39	1058
4			II	60	65	35	987
5			I	60	67	45	1220
6			II	60	71	44	1195
7			I	60	75	41	1107
8			II	60	78	43	1083
9			I	60	54	32	930
10			II	60	56	34	915

* The molar ratio for the catalyst : olefin : TBHP is 1 : 5000 : 5000. The reactions were carried out at 80°C.

In this process, the catalytic reaction may be prone to auto-retardation by coordination of the co-product *tert*-butanol to the molybdenum complex. *tert*-Butanol can compete with TBHP for coordination to the molybdenum center and form an inactive species that leads to the decreasing reaction rate [29].

ACKNOWLEDGMENTS

Financial assistance from the Qiqihar University is gratefully acknowledged.

REFERENCES

1. Haque, M.R., Ghosh, S., Hogarth, G., et al., *Inorg. Chim. Acta*, 2015, vol. 434, p. 150.
2. Szatkowski, L. and Hall, M.B., *Inorg. Chem.*, 2015, vol. 54, no. 13, p. 6380.
3. Hatnean, J.A. and Johnson, S.A., *Dalton Trans.*, 2015, vol. 44, no. 33, p. 14925.
4. Chatterjee, I., Chowdhury, N.S., Ghosh, P., et al., *Inorg. Chem.*, 2015, vol. 54, no. 11, p. 5257.
5. Sieh, D., Lacy, D.C., Peters, J.C., et al., *Chem. Eur. J.*, 2015, vol. 21, no. 23, p. 8497.
6. Rayati, S., Rafiee, N., and Wojtczak, A., *Inorg. Chim. Acta*, 2012, vol. 386, p. 27.
7. Alemohammad, T., Safari, N., Rayati, S., et al., *Inorg. Chim. Acta*, 2015, vol. 434, p. 198.
8. Kissel, A.A., Mahrova, T.V., Lyubov, D.M., et al., *Dalton Trans.*, 2015, vol. 44, no. 27, p. 12137.
9. Bagherzadeh, M., Ghanbarpour, A., and Khavasi, H.R., *Catal. Commun.*, 2015, vol. 65, p. 72.
10. Pranckevicius, C., Fan, L., and Stephan, D.W., *J. Am. Chem. Soc.*, 2015, vol. 137, no. 16, p. 5582.
11. Safin, D.A., Pialat, A., Korobkov, I., et al., *Chem. Eur. J.*, 2015, vol. 21, no. 16, p. 6144.
12. Bagh, B., McKinty, A.M., Lough, A.J., et al., *Dalton Trans.*, 2015, vol. 44, no. 6, p. 2712.
13. Rayati, S. and Salehi, F., *J. Iran. Chem. Soc.*, 2015, vol. 12, no. 2, p. 309.
14. Haque, M.R., Ghosh, S., Hogarth, G., et al., *Inorg. Chim. Acta*, 2015, vol. 434, p. 150.
15. Szatkowski, L. and Hall, M.B., *Inorg. Chem.*, 2015, vol. 54, no. 13, p. 6380.
16. Bagherzadeh, M., Amini, M., Parastar, H., et al., *Inorg. Chem. Commun.*, 2012, vol. 20, no. 1, p. 86.
17. Dupe, A., Hossain, M.K., Schachner, J.A., et al., *Eur. J. Inorg. Chem.*, 2015, no. 21, p. 3572.
18. Oliveira, T.S.M., Gomes, A.C., Lopes, A.D., et al., *Dalton Trans.*, 2015, vol. 44, no. 31, p. 14139.
19. Mirzaee, M., Bahramian, B., and Amoli, A., *Appl. Organomet. Chem.*, 2015, vol. 29, no. 9, p. 593.
20. Jones, M.M., *J. Am. Chem. Soc.*, 1959, vol. 81, no. 6, p. 3188.
21. Sheldrick, G.M., *SADABS*, Göttingen: Univ. of Göttingen, 1996.
22. Sheldrick, G.M., *SHELX-97, Program for Crystal Structure Solution and Refinement*, Göttingen: Univ. of Göttingen, 1997.
23. Sheldrick, G.M., *SHELXTL, Version 5*, Siemens, Madison: Industrial Automation Inc., 1995.
24. Geary, W.J., *Coord. Chem. Rev.*, 1971, vol. 7, no. 1, p. 81.
25. Gupta, S., Barik, A.K., Pal, S., et al., *Polyhedron*, 2007, vol. 26, no. 1, p. 133.
26. Ngan, N.K., Lo, K.M., and Wong, C.S.R., *Polyhedron*, 2012, vol. 33, no. 1, p. 235.
27. Bagherzadeh, M., Latifi, R., Tahsini, L., et al., *Polyhedron*, 2009, vol. 28, no. 12, p. 2517.
28. Nunes, C.D., Valente, A.A., Pillinger, M., et al., *Chem. Eur. J.*, 2003, vol. 9, no. 18, p. 4380.
29. Kuhn, F.E., Groarke, M., Bencze, E., et al., *Chem. Eur. J.*, 2002, vol. 8, no. 10, p. 2370.